

A geometry measurement system for a dimensional cone-beam CT

Benjamin A. Bircher, Felix Meli, Alain Küng, Rudolf Thalmann

Federal Institute of Metrology METAS, Laboratory for Length, Nano- and Microtechnology

Lindenweg 50, 3003 Bern-Wabern, Switzerland

e-mails: benjamin.bircher@metas.ch, felix.meli@metas.ch

Abstract

Computed tomography (CT) is increasingly used for dimensional high-resolution characterisation of small workpieces. Because there is demand for dimensional CT measurements and open questions concerning measurement uncertainty and traceability, METAS is developing and building a metrology CT system. The instrument will be used to characterise workpieces of millimetre dimensions and to study CT metrology in general. An overview of the system under development is given, with special focus on the developed CT geometry measurement system. Such an in situ geometry measurement system can be used to correct CT datasets and to study influencing factors on CT measurements.

Keywords: Cone-beam CT geometry, measurement system, degrees of freedom (DoF), dimensional metrology

1 Introduction

Industrial computed tomography is increasingly used for dimensional measurements [1]. It features many advantages, such as mapping of internal geometries, capturing the entire workpiece surface, and scan times independent of the number of measured geometrical features. Whereas in non-destructive testing resolution and contrast are key properties, dimensional measurements rely on distortion-free volume data. A variety of interfering factors impair reconstructing an ideal mapping of the investigated object. They originate from all CT components, their geometrical arrangement and the employed reconstruction and data analysis algorithms [2]. Consequently, important metrological issues such as traceability, measurement uncertainty, and standardisation remain not fully resolved [2]. To gain expertise in the field, METAS developed a high-resolution metrology CT. It is equipped with a novel geometry measurement system that monitors the arrangement of the components and enables separating geometry errors from errors originating from other sources, e.g. radiation-matter interactions. Furthermore, the geometry measurement system enables accurate and traceable determination of the source-object and source-detector distances, thus, rendering lengthy calibration measurements obsolete.

In this paper, an overview of the METAS-CT system is given, followed by a discussion on CT geometry and the required accuracy to render geometrical errors negligible. Subsequently, the geometry measurement system is presented and first characterisation measurements are shown.

2 Overview of the METAS-CT system

The METAS-CT system is designed for dimensional measurements on millimetre-sized workpieces. A microfocus X-ray tube (XWT-190-TCNF, X-RAY WorX) in combination with a 4k x 4k digital X-ray detector (XRD 1611 CP3, Perkin Elmer) render the system suitable for scanning workpieces smaller than 4 mm with a 1 μm voxel size. Air-bearing rotary and linear axes (LAB Motion Systems) ensure accurate and repeatable positioning of the workpiece and the detector. All guideway errors were comprehensively characterised [3]: In summary, the runout errors of the rotary stage were within $\pm 0.1 \mu\text{m}$ in typical scan heights. The straightness of the linear axes was better than $\pm 1.5 \mu\text{m}$ and the angular errors were below $\pm 7 \mu\text{rad}$. For optimal stability, only the minimally required number of degrees of freedom was implemented. Figure 1 shows the CT system before the implementation of the metrology system: The X-ray tube is stationary, whereas the detector can be moved in z-direction and the rotary stage, carrying the workpiece, in z- and y-direction. The y-displacement enables performing helical scan trajectories that fulfil the Tuy-Smith sufficiency condition [4]. Thus, the accuracy of dimensional measurements can be improved, provided that appropriate trajectory parameters are used [5]. For maximum temperature stability the system is housed in a walk-in radiation-shielded cabin that is connected to the in-house climate control and all CT control systems are installed outside. Furthermore, major heat sources, such as the X-ray tube and the detector, are equipped with active water-cooling systems.



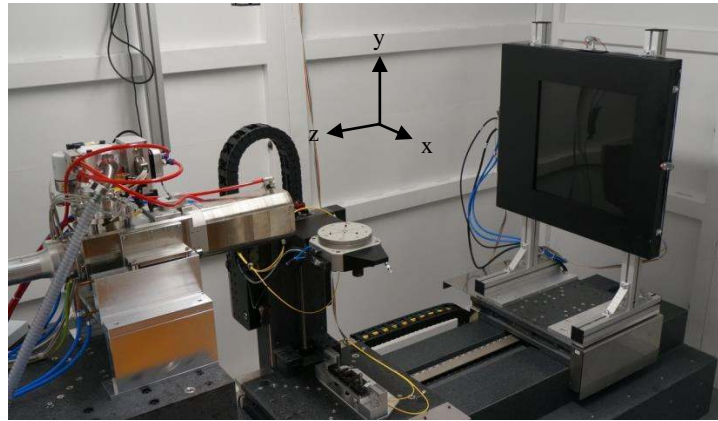


Figure 1: METAS-CT consisting of a microfocus transmission X-ray tube, an air-bearing positioning system and a 4k x 4k detector. The photograph shows the system before the implementation of the metrology system.

3 Ideal cone-beam CT geometry and required accuracy

The uncertainty of CT data is determined by a variety of factors. At high resolutions the geometry of the CT system, i.e. the relative position of the X-ray focal spot and the detector with respect to the object, can be a major source of error [6]. The ideal arrangement of these components is shown in Figure 2. The coordinate system origin is fixed in the centre of the detector plane, whose pixel rows and columns define the x- and y-axis, respectively. The source spot can be considered a point source, as long as it is smaller than the voxel size. Thus, its position is defined by 3 translational degrees of freedom (DoF). The object attached to the rotary axis has 3 translational and 3 rotational DoFs. Accordingly, the cone-beam CT system geometry is entirely characterised by 9 DoF. In the ideal case, the source is located on the magnification axis at $(x_s = 0, y_s = 0, z_s = SDD)$ and the object at $(x_o = 0, y_o = 0, z_o = SDD - SOD)$ exclusively being rotated around the y-axis into N rotary positions ($R_{ox} = 0, R_{oy} = N \Delta R_{oy}, R_{oz} = 0$). In a real CT-system all DoF deviate from their ideal position and, thus, these deviations should be taken into account.

Typically, some of the geometrical parameters are calibrated prior to high-accuracy scans using reference objects. However, the accuracy is limited by the employed calibration procedure and the geometrical parameters must remain stable during scanning of the reference and the object under investigation. This assumption holds for voxel sizes of several tens of micrometres. However, scanning parts with dimensions of a few millimetres results in voxel sizes of the order of $1 \mu\text{m}$. Thus, a positional accuracy and stability of the X-ray focal spot and the object of the order of $0.1 \mu\text{m}$ are required; in contrast the detector is less critical due to the magnification. Such high requirements are deteriorated by guideway errors of the employed axes and drift, caused by the fact that CT systems are large compared to the sample size and contain major heat sources, such as the X-ray tube and the digital detector. For this reason, we developed an in situ measurement system to determine and monitor the CT geometry. This supersedes lengthy calibration steps and enables accounting for non-repeatable errors and drift, which are major influence factors during high-resolution scans. The in situ measured deviations from the ideal geometry can eventually be used for corrections, either mechanically, through projection image processing or during reconstruction.

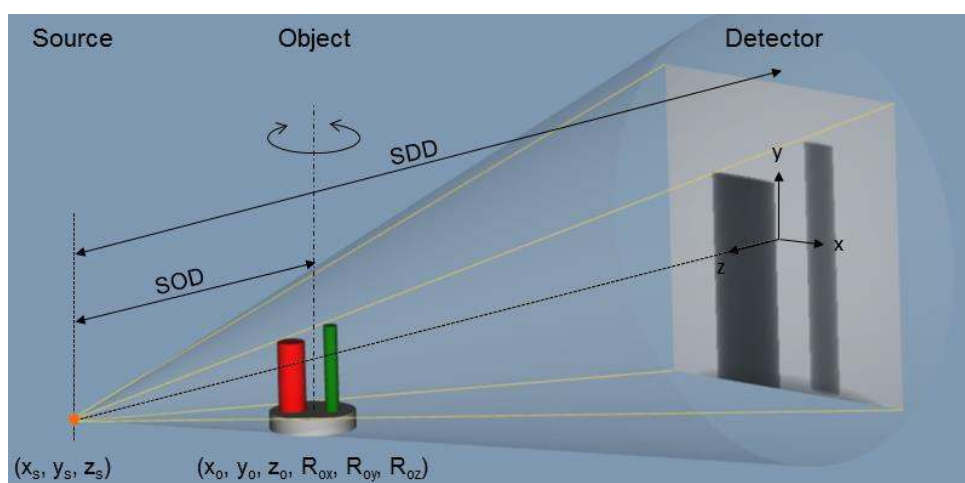


Figure 2: The geometry of a cone-beam CT consists of 9 degrees of freedom (DoF) under the assumption of a point source and an ideal detector. The X-ray source coordinates are (x_s, y_s, z_s) , the object is positioned at (x_o, y_o, z_o) with rotation angles (R_{ox}, R_{oy}, R_{oz}) with respect to the detector reference system.

4 CT geometry measurement system

4.1 Concept

To determine the 9 DoF of a CT system, described in section 3, at least 9 separate sensors are required. Here, the 9 DoF are derived from 22 measured position values. For example, it is difficult to determine the source-detector distance on the magnification axis, since it would require the sensor system to be placed in the primary X-ray beam. As a solution, multiple interferometers can be placed around the magnification axis and the desired position, in this case the detector centre position, can be calculated. Additionally, air pressure, humidity, and 20 temperature values are recorded and used for further corrections.

The concept of the cone-beam CT geometry measurement system is shown in Figure 3. It consists of a metrology frame (in blue) close to the X-ray tube. The frame is not in contact with the tube to avoid heat flowing into it and also to simplify tube maintenance. To relate the position of the X-ray tube target to the metrology frame, a dedicated X-ray tube measurement system was developed that is described below. The sample stage and detector position are monitored by fibre based interferometers (measurement direction along the laser beam axis) and home-built straightness sensors (measurement direction perpendicular to the laser beam axis). Traceability to the SI is provided by calibrating the laser wavelengths and the various sensors for straightness, air pressure, temperature and humidity. However, in CT systems the detector and X-ray tube target lack mechanical reference points. Furthermore, other effects, e.g. the penetration depth into the scintillator [7], can render their position dependant on the used X-ray energy. The first challenge can be addressed by recording X-ray projections of a calibrated artefact and use an appropriate analysis to determine the absolute system geometry. One or multiple index sensors on the translation stages can then be used to set the measurement system to zero. The second effect can be addressed by either carefully characterising it or considering it in the measurement uncertainty estimation. Below, the used sensor types are presented and a detailed description of the measurement systems monitoring the X-ray tube and the sample stage is given.

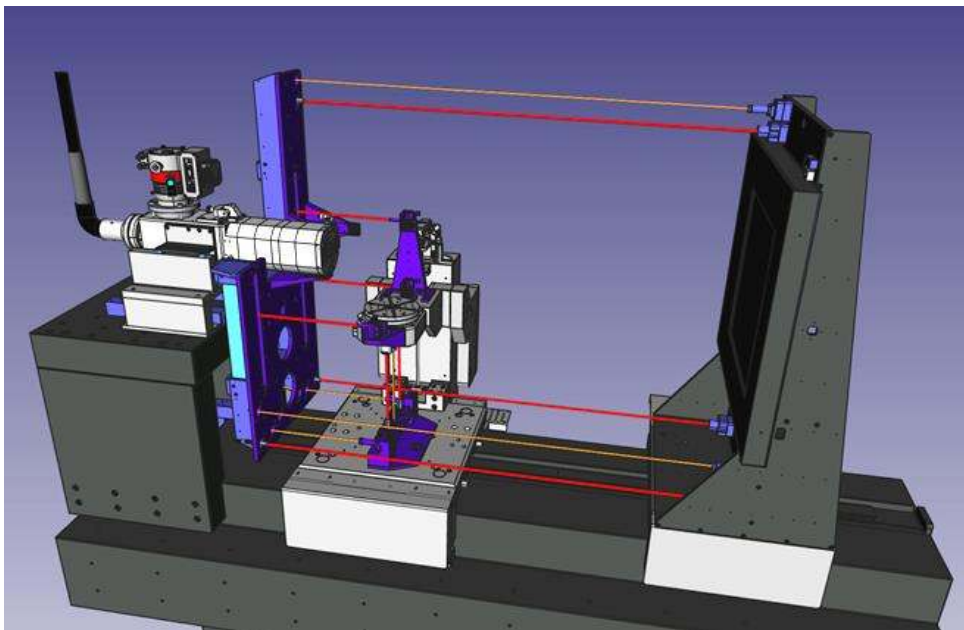


Figure 3: Concept of the cone-beam CT geometry measurement system used to determine the position of the X-ray tube (left), sample (middle) and detector (right): The system consists of eight fibre interferometers (red laser beams), five straightness sensors (orange laser beams), an X-ray tube measurement system, and an index sensor that are all referred to a metrology frame (blue frame on the left).

4.2 Sensor types

4.2.1 Fibre interferometers

The used interferometers are fibre-coupled low finesse Fabry-Pérot type with a nominal wavelength of 1530 nm (FPS3010, attocube). First, the absolute wavelength and wavelength stability of the three instruments was measured with a calibrated wavemeter (Burleigh, WA-1500). The absolute wavelength of all three devices was within (1530.3712 ± 0.0001) nm and the stability was better than 10^{-8} over 1 hour. Furthermore, the refractive index of air, which changes the wavelength [8], must be considered. Thus, an air temperature, humidity and pressure measurement system was implemented. Finally, the non-linearity of the fringe interpolation of the interferometers was measured against a plane mirror that was displaced using a piezo stage with a capacitive encoder. It ranged from < 10 nm to 100 nm, depending on the setting for the maximum working range, which changes the wavelength modulation amplitude that is used for the quadrature signal. In conclusion, the accuracy of the employed interferometers is sufficient to measure the corresponding distances within 0.1 μm .

The interferometers are used to determine the source-object (SOD) and source-detector (SDD) distances, which determine the magnification (SDD/SOD) and the cone-beam opening angle. Since multiple interferometers are used, these values can be projected on the magnification axis by taking weighted averages, thus, following the Abbe principle. Furthermore, angular deviations can be measured by using the same interferometers differentially.

4.2.2 Image sensor for straightness and displacement measurements

For straightness measurement and monitoring the X-ray tube head, a sensor based on a CMOS camera chip has been developed. By determining the centre of the laser beam on the camera (Figure 4a), displacements perpendicular to the beam axis can be measured. Commonly, four-quadrant diodes are used for this task, but to be implemented as straightness sensor, they need to be calibrated and operated in the linear region. An image sensor can be used instead to locate the beam centre with sub-pixel accuracy. The pixels, which are manufactured with the highest lithographic precision, are thereby acting as a 2D-scale. The ease of use and moderate pricing of digital cameras make them superior over four-quadrant diodes. Their only drawback is the power dissipation, which could lead to thermal drifts of the CMOS chip position.

Monochrome CMOS cameras (daA1280-54um, Basler), with a 1.2 M pixel chip, $3.75 \mu\text{m}$ square pixel size, and 1.2 W power consumption, were used. The laser beam was issued from a single-mode optical fibre pigtailed to a 639 nm laser diode. Prior to a measurement, the camera sensitivity and exposure time is optimized to obtain the best signal-to-noise ratio without any saturation. Images were recorded at 10 fps. To render the sensor insensitive to inhomogeneous background illumination, an intensity threshold was implemented. The centre of the beam is determined by calculating the centre of gravity of the grey values, resulting in an x- and y-position. 10 position values are box-averaged resulting in a sensor bandwidth of about 1 Hz. Two configurations are employed: Either the fibre end shining directly onto the chip at a constant distance between 1 and 5 mm for the X-ray tube position measurement system; or the fibre end was fitted with an aspheric lens collimator in order to form a $\varnothing 1 \text{ mm}$ Gaussian beam that can be measured over a range of 2 m along the beam axis for the straightness sensors. It is emphasised that a near-perfect Gaussian beam profile is key for the accuracy of the sensor.

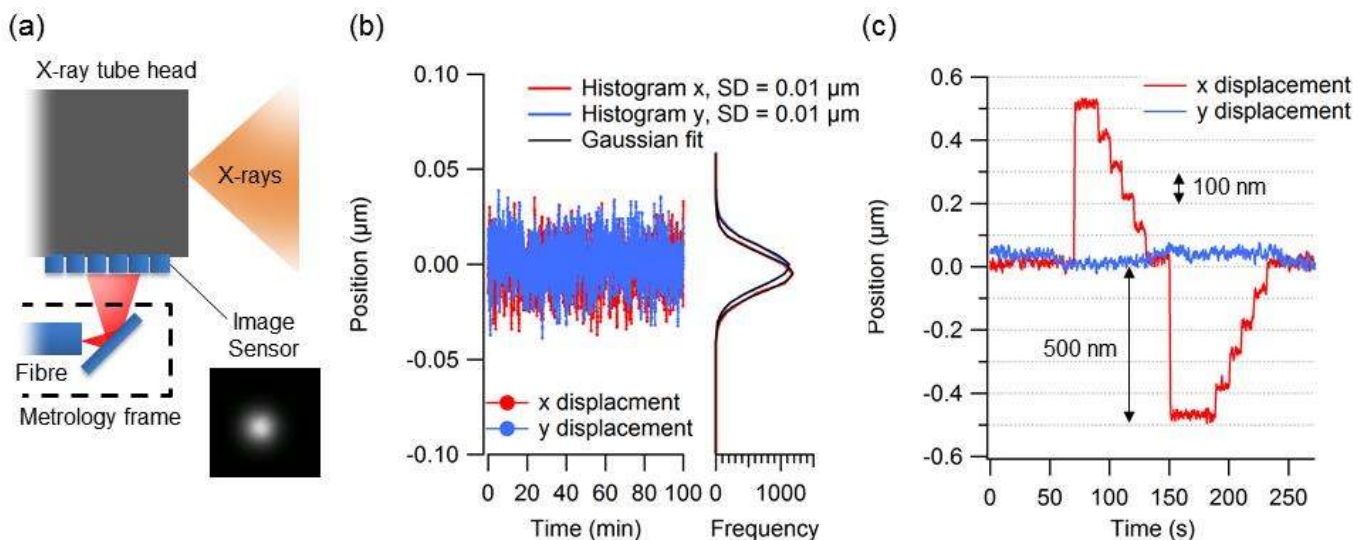


Figure 4: Image sensor based measurement system: (a) Principle: A laser beam from a single-mode fibre is incident on a CMOS camera chip attached to the X-ray tube. The centre of the beam is determined and equals the lateral displacement between the X-ray tube and the incident laser beam. (b) Stability measurement: The intrinsic noise floor of the sensor was 10 nm (1σ). (c) Displacements of 100 nm and 500 nm were realised using a linear stage and accurately measured by the sensor.

4.3 Results

4.3.1 X-ray tube position measurement system

The absolute position and stability of the X-ray focal spot is a key requirement for accurate CT scans. It is defined by the point of incidence where electrons are decelerated in the target material, typically tungsten, and partially converted into X-rays [1]. Direct measurement of the point of incidence of the electron beam on the target proves difficult. Therefore, high-density apertures are used in the employed transmission type X-ray tube, to centre the electron beam relative to the X-ray tube axis. The developed X-ray tube measurement system uses the position of such aperture as a mechanical reference point. Two image sensors (see section 4.2.2) are attached on the side and bottom of the X-ray tube head close to the target surface. Two cantilever arms, attached to the metrology frame, carry a fibre and a 45° mirror to deflect the laser beam on the image sensors (see Figure 4a). Thus, the position of the X-ray tube aperture relative to the metrology frame can be determined. Consequently, the position of the focal can be determined within its stability relative to the X-ray tube.

In order to test the fundamental accuracy of the image sensor based lateral displacement measurement, the bare fibre end was positioned about 2 mm from the camera chip surface. The noise level of the system was less than 10 nm (1σ , see Figure 4b) and the drift is negligible when adhering to a warm-up period. During warm-up the observed drift was below $0.5 \mu\text{m}$, thanks to the central position of the chip in respect to the camera mounting screws. In a second experiment, the fibre end was mounted on a displacement stage. The position of the stage was actively controlled on its integrated line scale and a trajectory of 500 nm steps and 100 nm steps was programmed. Figure 4c shows the displacement of the centre of the laser beam measured by the image sensor. The results show that the stage follows the programmed trajectory, which was accurately measured by the image sensor.

Since the stability of the focal spot relative to the X-ray tube is critical for the measurement principle, it was determined by attaching a steel sphere mounted on a CFRP (carbon fibre reinforced polymer) rod directly to the tube head (Figure 5a). 2160 X-ray projections of the steel sphere were recorded over 9 hours operating the X-ray tube in microfocus mode at 120 kV with a target power of 6 W. The projections were analysed using FIJI [9]: An ISO50 threshold was used to segment the sphere and the centre of gravity of the resulting binary map was calculated to determine the sphere position in pixels (Figure 5b). The lateral focal spot position is geometrically related to the sphere position on the detector:

$$x_{\text{spot}} = \frac{x_{\text{sphere,det}}}{M - 1}$$

where x_{spot} is the focal spot position relative to the X-ray tube head, $x_{\text{sphere,det}}$ is the sphere position in the projection, and M is the magnification. The magnification was determined for each projection by $M = D_{\text{sphere,det}}/D_{\text{sphere}}$, where $D_{\text{sphere,det}}$ is the sphere diameter in the projection image, and D_{sphere} is the sphere diameter (1.59 mm).

Figure 5c shows the X-ray focal spot position over 9 hours. To allow the sphere to mechanically settle from drift, a warm-up period, where the magnification changed from 123.4 to 123.3, corresponding to a source-object displacement of $6 \mu\text{m}$, was adhered to. Subsequently, the lateral stability of the focal spot relative to the sphere was better than $0.6 \mu\text{m}$. Thus, the focal spot position can be correlated to the signals from the measurement system within this accuracy.

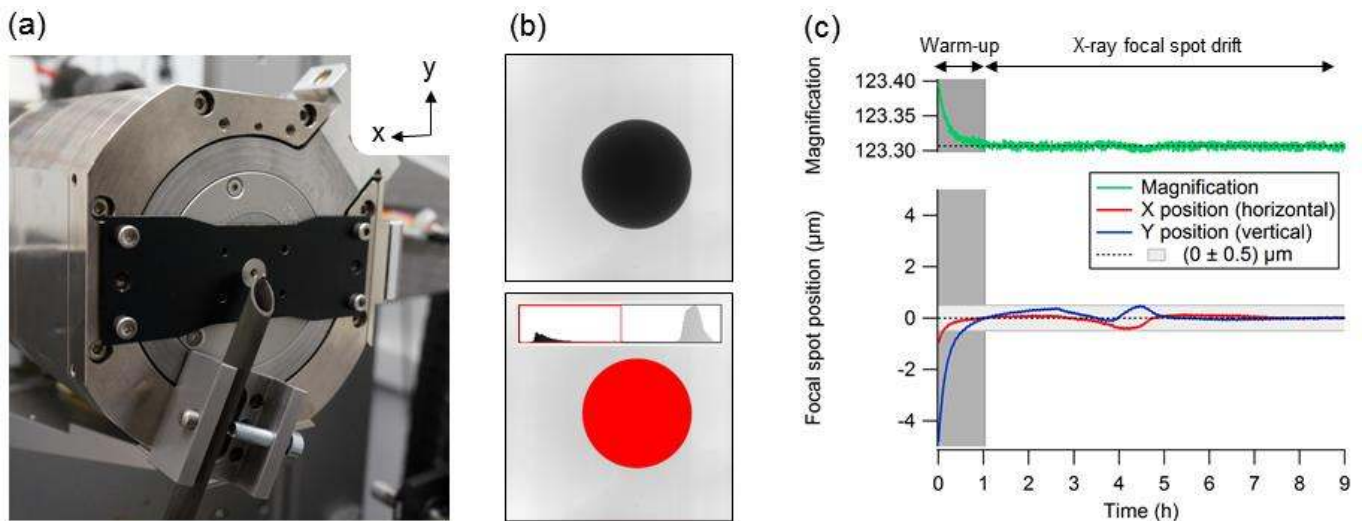


Figure 5: Measured X-ray focal spot stability relative to the tube head. (a) Photograph of the setup: A $\varnothing 1.59 \text{ mm}$ steel sphere attached to a CFRP rod is fixed at the tube head. (b) The X-ray projections (top) of the sphere were segmented (bottom, red area) to determine its position; the inset in the bottom image shows the segmented histogram. (c) The actual magnification and X-ray focal spot drift in the lateral directions are shown. Since the measurement relies on the mechanical stability of the sphere mounting, a warm-up period was adhered to.

4.3.2 Sample stage measurement system

The sample stage, which is used to displace the object, has 6 DoF. Three of them are adjustable: it can be rotated (R_y) to implement the circular scan trajectory and be translated in two directions (y and z). Its measurement system is shown in Figure 6. Because the two linear stages are in series, not all parameters can be directly referred to the metrology frame. The angles R_x and R_y and the position along the magnification axis z can be determined using three interferometers against two plane mirrors. In contrast, the angle R_z and displacements x and y are determined using an intermediate step: Two straightness sensors are used to determine the roll and straightness error motion of an intermediate metrology frame placed on carriage Z1. From there, another straightness sensor and two interferometers measure the straightness and pitch error of the sample stage. By combining those values, the sample stage position in relation to the metrology frame can be determined.

Measurements to evaluate the straightness sensors and interferometers of the sample stage are compared to values obtained using complementary classical measurement methods described in Reference [3]: Tactile measurements on a ceramic straight

edge were used to determine the straightness and electronic levels for the angular errors. The results are shown in Figure 7. The values coincide well, however there are some deviations smaller than $\sim 0.3 \mu\text{m}$. They are most likely because the measurements were not performed at the same time. Therefore, they could be caused by the long-term non-repeatable errors of the guideways.

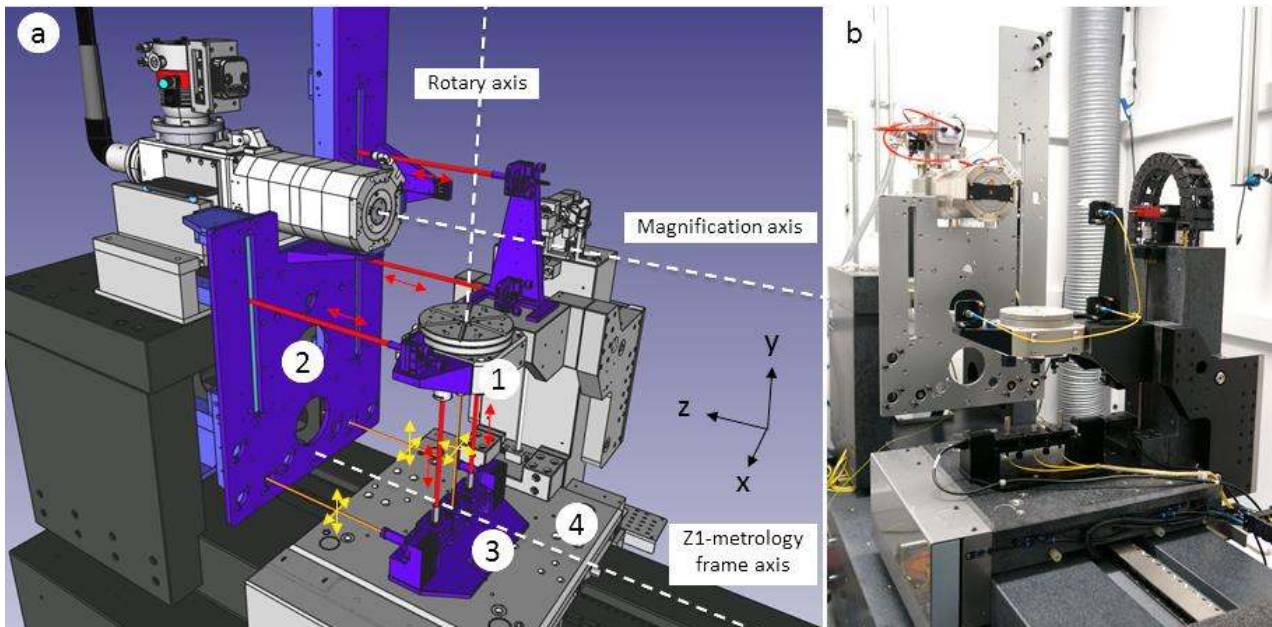


Figure 6: (a) Detail of the sample stage measurement system: To relate the sample stage (1) position to the metrology frame (2), an intermediate metrology frame (3) on the Z1-stage (4) is used. Interferometer laser beams are depicted in red and straightness sensors in orange; the corresponding measurement directions are indicated. The point of interest is the intersection between the rotary and the magnification axis. (b) Photograph of the implementation.

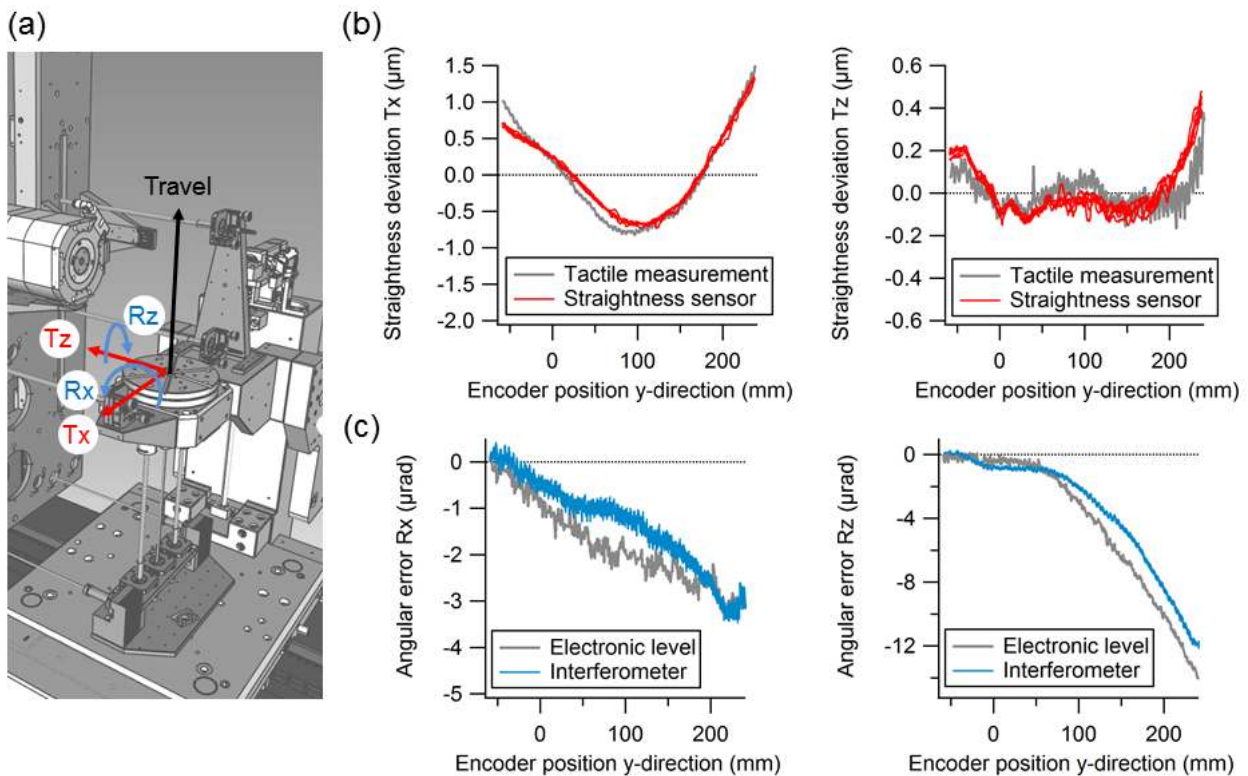


Figure 7: Evaluation of the CT geometry measurement system (coloured curves) against reference measurements (grey curves, data from Reference [3]): (a) Coordinate system for the guideway error measurements of the sample stage. (b) Home-built straightness sensors (red curves) compared to tactile measurements against a straight edge (grey curves). (c) Angular measurements using the differential interferometers (blue curves) and electronic levels (grey curves).

5 Conclusion and outlook

In this paper, a geometry measurement system for a high-resolution metrology CT is presented. The system enables monitoring the full CT geometry during scans with sub-micrometre accuracy. To locate the absolute position of the X-ray focal spot, the rotary axis and the detector, the system still needs to be calibrated through X-ray projections of an object. Therefore, appropriate reference objects will be developed.

Subsequently, the system will be used to correct CT data, e.g. by using the method described in Reference [10]. It furthermore enables studying influence factors on the CT geometry, such as heat sources that are abundant in CTs, or to separate the geometry errors from other interfering factors.

Acknowledgements

The authors acknowledge all members the laboratory length, nano- and microtechnology who contributed to the project and the members of the mechanical workshop, the laboratory for ionising radiation, and the laboratory photonics, time and frequency at METAS for their support.

References

- [1] De Chiffre L, Carmignato S, Kruth J P, Schmitt R and Weckenmann A 2014 Industrial applications of computed tomography *CIRP Ann. - Manuf. Technol.* **63** 655–77
- [2] Kruth J P, Bartscher M, Carmignato S, Schmitt R, De Chiffre L and Weckenmann A 2011 Computed tomography for dimensional metrology *CIRP Ann. - Manuf. Technol.* **60** 821–42
- [3] Bircher B A, Meli F, Küng A and Thalmann R 2017 Characterising the Positioning System of a Dimensional Computed Tomograph (CT) Submitted to MacroScale - Recent developments in traceable dimensional measurements
- [4] Muders J, Hesser J, Lachner A and Reinhart C 2011 Accuracy evaluation and exploration of measurement uncertainty for exact helical cone beam reconstruction using katsevich filtered backprojection in comparison to circular Feldkamp reconstruction with respect to industrial CT metrology *Int. Symp. Digit. Ind. Radiol. Comput. Tomogr.*
- [5] Aloisi V, Carmignato S, Schlecht J and Ferley E 2016 Investigation on metrological performances in CT helical scanning for dimensional quality control 6th Conference on Industrial Computed Tomography, Wels, Austria (iCT 2016)
- [6] Ferrucci M, Leach R K, Giusca C, Carmignato S and Dewulf W 2015 Towards geometrical calibration of x-ray computed tomography systems—a review *Meas. Sci. Technol.* **26** 92003
- [7] Illemann J and Bartscher M 2017 X-ray spectrum dependence of the magnification of cone-beam CT 7th Conf. Ind. Comput. Tomogr. Leuven, Belgium (iCT 2017)
- [8] Bönsch G and Potulski E 2003 Measurement of the refractive index of air and comparison with modified Edl n's formulae *Metrologia* **35** 133–9
- [9] Schindelin J, Arganda-Carreras I, Frise E, Kaynig V, Longair M, Pietzsch T, Preibisch S, Rueden C, Saalfeld S, Schmid B, Tinevez J Y, White D J, Hartenstein V, Eliceiri K, Tomancak P and Cardona A 2012 Fiji: An open-source platform for biological-image analysis *Nat. Methods* **9** 676–82
- [10] Meli F, Bircher B A, Blankenberger S, Küng A and Thalmann R 2018 A cone-beam CT geometry correction method based on intentional misalignments to render the projection images correctable submitted to 8th Conference on Industrial Computed Tomography, Wels, Austria (iCT 2018)